Best students papers in Vienna showcase young talent coming through

Three student papers have been chosen as the best submissions for the EAGE Annual Conference in Vienna. The work – covering pore scale visualization of polymer viscoelasticity, process-based modelling of sediment distribution in fluvial crevasse splays, and using effective medium theory to better constrain full wave inversion – is a testament to the great young talent coming through in the world of geoscience.

Using effective medium theory to better constrain full waveform inversion

M. Afanasiev[1*], C. Boehm[1], D. May[1] and A. Fichtner[1]

In seismic tomography, we are interested in finding a model $\mathbf{m}$ (spatial dependence omitted for clarity) which minimizes an objective function, and which also satisfies some broad physical constraints (e.g. velocities must be greater than zero, Poisson's ratio must lie within a certain range, etc.). Even with these constraints, the null space of the seismic inverse problem is extremely large, and to further constrain this space some form of regularization is required. Given a forward modelling operator $\mathbf{g}$ and a dataset $\mathbf{d}$, the optimization problem then becomes

$$\underset{\mathbf{m}\in M}{\operatorname{argmin}} \quad ||\, g(\mathbf{m}) - \mathbf{d}\,|| + \alpha\Omega[\mathbf{m}], \qquad (1)$$

where we solve for the optimal model $\mathbf{m}$ that lies within the constrained model space M. This model is considered optimal if it minimizes a measure of data misfit $g(\mathbf{m})$-$\mathbf{d}$, in addition to minimizing a α- weighted measure of regularization $\Omega[\mathbf{m}]$, which may take one of many forms (i.e. smoothness, proximity to an a-priori model, sparsity, etc.). While much work on null space reduction is aimed at exploring the regularization term in Equation 1, an often subjective process, this study attempts to reduce the null space by placing additional objective physical constraints on the set of acceptable models M.

Theory

High-resolution seismic imaging techniques, such as full waveform inversion (FWI), are typically performed in a multi-scale manner (Bunks et al., 1995). In practice, this means that inversions begin with low-frequency data, with higher frequency components being added as the low-frequency components converge. In the model domain, these higher frequency components serve to add wavenumber perturbations which are on the order of their wavelength: as higher frequencies are included, smaller heterogeneities are uncovered (Virieux and Operto, 2009). The intuitive basis behind the work presented here focuses on the fact that the low frequency/wavenumber components converge first, and exploits this fact to better condition the inversion at higher frequencies. Reformulating this in the language used in the introduction: we are adding additional constraints to the space M in Equation 1, with the constraints being that the already-converged low frequency/wavenumber components should not change.

To formalize these constraints, we turn to effective medium theory (Backus, 1962; Capdeville et al., 2010; Jordan, 2015). Effective medium theory describes how the elastic response of a medium is related across length scales. In general, these relationships are integral equations of the form

$$\mathbf{m}^{\star} = \langle \mathbf{m} \rangle \equiv \frac{1}{\lambda}\int_{\lambda} \mathbf{m}(\mathbf{x})\, d\mathbf{x} \qquad (2)$$

Here $\mathbf{m}^*$ is the 'effective' parameter seen by lower frequency signals, $\mathbf{m}$ is the 'fine-scale' parameter seen by higher frequency signals, and λ is the 'unit cell'. Length scales much smaller than λ are regarded as belonging to the fine-scale of the medium.

We can add these constraints to the inverse problem by defining a feasible set $\mathbf{M} \subset M$, within which all model updates $\mathbf{m}_u$ to a model with a converged low-wavenumber component $\mathbf{m}^*$ must lie:

$$\mathbf{M} = \left\{ \mathbf{m}_u \,|\, (1-\epsilon)\mathbf{m}^{\star} \leq \langle \mathbf{m}_u \rangle \leq (1+\epsilon)\mathbf{m}^{\star} \right\} \qquad (3)$$

where ε is some small positive number. Now, we can check whether or not a

[1] *ETH Zurich.*
[*] *Corresponding author, E-mail: michael.afanasiev@erdw.ethz.ch*

proposed model update $\mathbf{m}_u$ (such as one coming from an iteration of FWI) lies within the feasible set or not. If it does not, we can enforce conformance by projecting the update onto the feasible set, using the Jacobian of Equation 3 (Wächter and Biegler, 2006). With feasibility ensured, we now solve an auxiliary optimization problem:

$$\underset{\mathbf{m}\in\mathbf{M}}{\text{argmin}} \quad ||\mathbf{m}-\mathbf{m}_u||+\alpha\Omega[\mathbf{m}] \qquad (4)$$

where $\mathbf{m}_u$ is the originally proposed model update, and $\alpha\Omega[\mathbf{m}]$ is again some weighted measure of regularization. Note here that owing to the constraints, any subjective regularization in Equation 4 will not affect the convergence of the model at scales larger than the unit cell. Also note that this auxiliary problem does not involve additional wavefield simulations, and is comparatively cheap with respect to a FWI update (especially when considering multiple sources).

Results

As a proof of concept, we turn to the simple case of layered media, and construct the synthetic crosshole FWI experiment illustrated in Figure 1. This set-up allows us to use the analytical results from Backus (1962) to solve Equation 2. The true model, shown in Figure 1a consists of a layered half-space. Elastic waves are propagated through this model from a source (black circle), to a string of receivers (black line), to create a set of 'observed' data. Our starting model for FWI is a Backus-averaged version of the true model (Figure 1b). We then perform an un-regularized FWI update, using L_2 waveform differences as a misfit measure, to obtain the raw update in Figure 1c. Projecting this update on to the feasible set in Equation 3, with ε = 0.01, and solving the auxiliary problem in Equation 4 results in an improved update, as shown in Figure 1d. The majority of the artefacts appearing in Figure 1c are removed.

Conclusions

This work has recast seismic inversion as a constrained optimization problem, with constraints derived from effective medium theory. This formulation allows us to use the multi-scale convergence typical of such problems to extract physically meaningful portions of raw gradient updates, and to perform objective physics-based regularization. Tests on layered media show encouraging results, with current work focusing on more complex media, and engineering-scale applications.

References

Backus, G.E. [1962]. Long-wave elastic anisotropy produced by horizontal layering. *Geophysical Journal International*, **67**, 4427–4440.

Bunks, C., Saleck, F.M., Zaleski, S. and Chavent, G. [1995]. Multiscale seismic waveform inversion. *Geophysics*, **60**, 1457–1473.

Capdeville, Y., Guillot, L. and Marigo, J.J. [2010]. 1-D non periodic homogenization for the wave equation. *Geophysical Journal International*, **181**, 897–910.

Jordan, T.H. [2015]. An effective medium theory for three-dimensional elastic heterogeneities. *Geophysical Journal International*, **203**(2), 1343–1354.

Virieux, J. and Operto, S. [2009]. An overview of full waveform inversion in exploration geophysics. *Geophysics*, **74**, WCC127–WCC152.

Wächter, A. and Biegler, L. [2006]. On the implementation of an interior-point filter line-search algorithm for large-scale nonlinear programming. *Mathematical Programming*, **106**, 25–57.

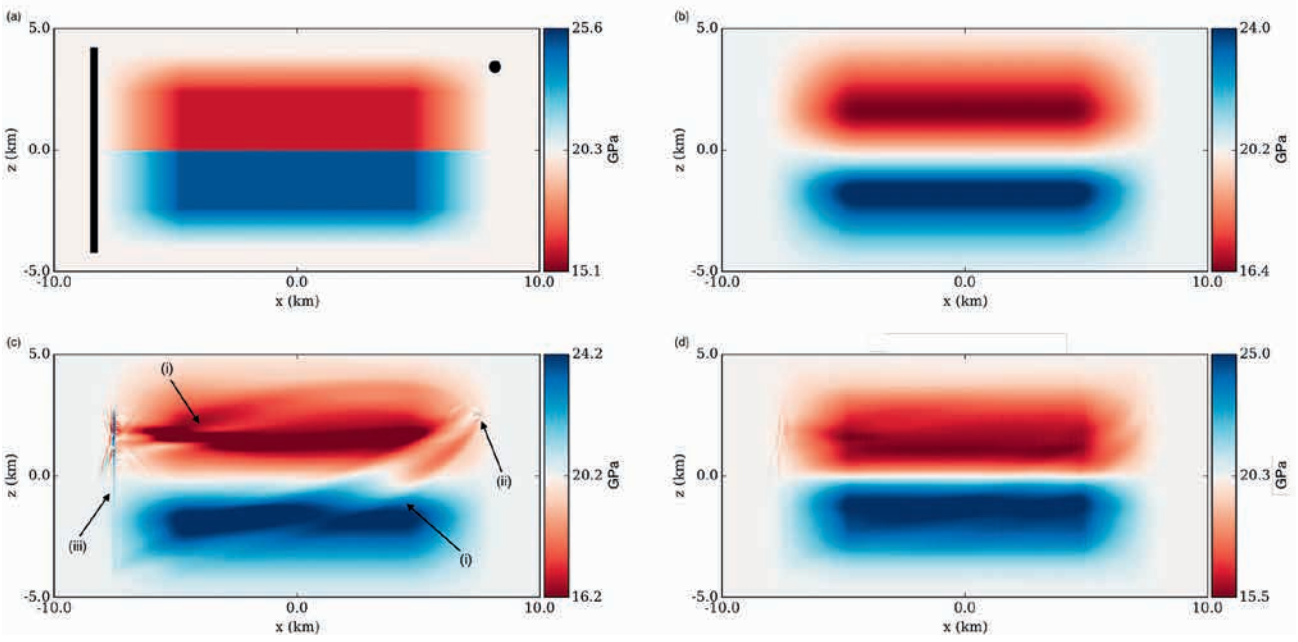

Figure 1 *(a) True model (μ), source at black circle, receivers along black line; (b) Starting model (L [Backus parameter]); (c) Proposed update (μ), showing strong artefacts, including those from (i) incomplete data coverage, (ii) source effects, and (iii) receiver effects; (d) Projected update (μ).*

Process-based modelling of sediment distribution in fluvial crevasse splays

A.B. Sandén[1*], H.T.W. Boerboom[1], M.E. Donselaar[1], J.E.A. Storms[1], K.A. van Toorenenburg[1], H. van der Vegt[1] and G.J. Weltje[2]

The mature North Sea gas province suffers from a decline in the production of gas from conventional reservoirs. Exploitation of unconventional resources could prolong the gas supply in the future. Previous work identified low net-to-gross fluvial strata as a possible secondary target (Donselaar et al., 2011). However, these intervals are traditionally not classified as reservoir rock in the conventional characterisations.

For the assessment of the economic risks associated with the uncertainties of these unconventional crevasse splay reservoirs, an objective prediction of the sediment size and its spatial distribution are required. Sparse areal data availability for reservoir models commonly result in the use of stochastic interpolation. Numerical models offer the possibility to support these methods with proven physical concepts.

The aim of this study is to create a grain-size distribution model of a crevasse splay deposit on a low-gradient coastal plain in a semi-arid endorheic basin. A process-based model combined with conventional outcrop data is used to create a solid sediment distribution predictive model.

Method

Input parameters and the validation data sets for the process-based model were derived from outcrop studies in the present-day Río Colorado fluvial system in the Altiplano Basin, Bolivia. Quantitative data sets of the channel/floodplain morphology (Donselaar et al., 2013), discharge models (Li et al., 2014), and grain-size distribution in crevasse splays were used for the present study.

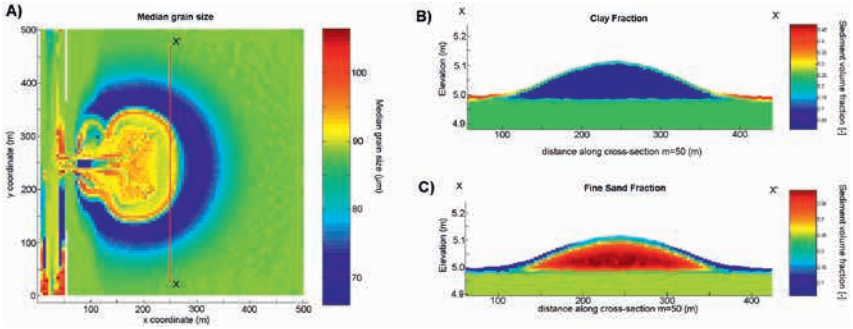

Figure 1 *Example of a model simulation output. A) The areal grain-size distribution. The values are vertically averaged over the thickness of the splay deposit. B) Cross section X-X'. The core of the crevasse splay consists predominantly of sand with minor clay deposition along the margins of the splay. A clay drape forms during the final stage of the crevasse splay deposition. C) The same cross section as in B, showing the fine sand fraction. A clear fining upward trend is visible.*

For the simulation of a single crevasse splay sediment body, the numerical process-based model Delft3D software was used (Figure 1). It uses a finite-difference scheme to solve for the Navier-Stokes equations, simulating fluid flow, sediment transport, and morphological changes (Roelvink and Van Banning, 1995; Lesser et al., 2004).

Results

The model shows an overall fit with the grain-size data from the fieldwork data. It captures the general trends, but it does not capture all the variations present in the measured data. The mean grain sizes of the simulated surface sediments for a single flood event show a clear trend. Grain size decreases with increasing distance from distributary channels (Figure 1). This is in line with the physical concept of decreasing sediment size for decreasing flow energy. Significant input parameters are the total discharge, sediment input and the levee composition.

Discussion

A numerical model can be a valuable aid to reservoir description. Combining a model that applies hydrodynamics and sediment transport, with validation field-based data, we use the individual strengths of different methods (Shenton, 2004). This concept will be tested in the future. Data from outcrop analogues in the Huesca fluvial fan (Nichols and Fisher, 2007) will be used to explore the general applicability of the model.

Industry standard reservoir modelling software offer stochastic algorithms to simulate the placement and dimensions of fluvial objects. Observed grain size trends can be used to populate individual crevasses splays within a static model. Dynamic flow calculations will be used to assess the economic risks. The numerical parameters of the process-based model will be optimized to ensure a representable upscaling.

Conclusion

Process-based models can be used to support and confirm sediment trends

[1] *Delft University of Technology.*
[2] *KU Leuven.*
[*] *Corresponding author, E-mail: absanden@gmail.com*

and depositional mechanisms of a crevasse splay. The combination of numerical and discrete field data provides a sound case for sediment distribution predications. Simulations, however, still have a limited accuracy.

Acknowledgements

This study is supported by ENGIE E&P NL and EBN. Yadir Torres Carranza and Niels Noordijk are gratefully acknowledged for their contributions in data acquisition. Facilities for the grain-size analysis were provided by the VU University Amsterdam.

References

Donselaar, M.E., Cuevas Gozalo, M.C. and Moyano, S. [2013]. Avulsion processes at the terminus of low-gradient semi-arid fluvial systems: lessons from the Río Colorado, Altiplano endorheic Basin, Bolivia. *Sedimentary Geology*, **283**, 1-14.

Donselaar, M.E., Overeem, I., Reichwein, J.H.C. and Visser, C.A. [2011]. Mapping of fluvial fairways in the Ten Boer Member, Southern Permian Basin. *The Permian Rotliegend of The Netherlands,* SEPM special publication, **98**, 105-117.

Nichols, G.J. and Fisher, J.A. [2007]. Processes, facies and architecture of fluvial distributary system deposits. *Sedimentary Geology*, **195**, 75-90.

Lesser, G.R., Roelvink, J.A., Van Kester, J.A.T.M. and Stelling, G.S. [2004]. Development and validation of a three-dimensional morphological model. *Coastal engineering*, **51** (8), 883-915.

Li, J., Donselaar, M.E., Aria, S.E.H., Koenders, R. and Oyen, A.M. [2014]. Landsat imagery-based visualization of the geomorphological development at the terminus of a dryland river system. *Quaternary International*, **352**, 100-110.

Roelvink, J.A. and Van Banning, G.K.F.M. [1995]. Design and development of DELFT3D and application to coastal morphodynamics. *Oceanographic Literature Review*, **11** (42), 925.

Shenton, A.K. [2004] Strategies for ensuring trustworthiness in qualitative research projects. *Education for information*, **22** (2), 63-75.

Pore-scale visualization of polymer viscoelasticity using particle tracing in glass-silicon-glass micromodels

A. Rock[1*], R.E. Hincapie[1], J. Wegner[1], H. Födisch[1] and L. Ganzer[1]

The several mechanisms concerning viscoelasticity of aqueous polymer solutions used for EOR are in some ways misunderstood. Increasing viscosity as a result of increasing shear rate – known as 'Shear Thickening' – is one of those. Flooding experiments in Glass-Silicon-Glass (GSG) micromodels, resembling real porous media, contribute to understanding of elastic turbulences, which people suspect is the main reason for this phenomenon, apart from viscoelastic properties. The focus of this work is on the investigation of viscoelasticity of polymer solutions by using particle tracing focusing on streamlines visualization in the pores during the flood. Photos and videos record different injection flow rates. Videos and pressure data are used subsequently for qualitative and quantitative flow behaviour characterization, with focus on elastic turbulence originated by injected polymer solutions. In addition, results are compared to the behaviour of a Newtonian fluid.

Experimental approach

Visualizations of the flow patterns relies on streak videos and photos generated from them. For this purpose, 1µm tracers (with polystyrene matrix particles composition) are added to the polymer solutions. The optical setup consists of an inverted epi-fluorescence microscope (Imager.Z2m, Zeiss) equipped with a CCD camera. Micromodels were placed under the microscope and were continuously illuminated, while path line images were acquired using a LD 'Plan-Neofluar' 20x/0,40 (D=0-1,5 mm) microscope objective and long exposure times to obtain a visual fingerprint of the flow patterns in the focused centre plane. The quarter-of-a-five-spot micromodel is connected with a syringe pump by stainless steel pipes

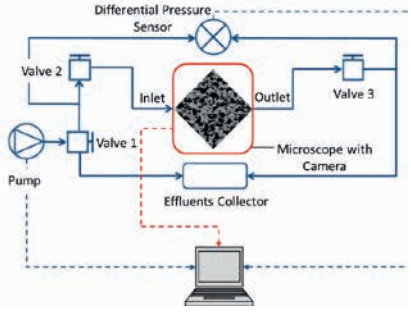

Figure 1 *Scheme of experimental set-up used for streamline visualization and single-phase micromodel polymer flooding.*

[1] *Clausthal University of Technology.*
[*] *Corresponding author, E-mail: alexander.rock@tu-clausthal.de*

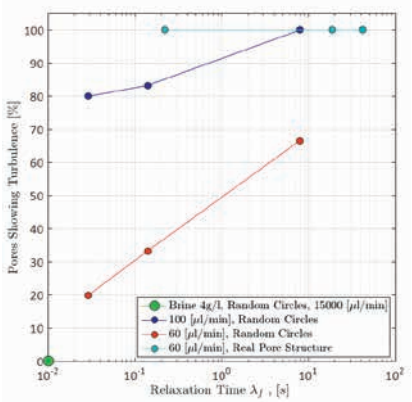

Figure 2 *Polymers with different characteristic relaxation time (λf) show a correlation between viscoelasticity and elastic turbulence. Variation of pore geometry and flow rate shows an influence on the flow behaviour, too. (λf of brine is 0).*

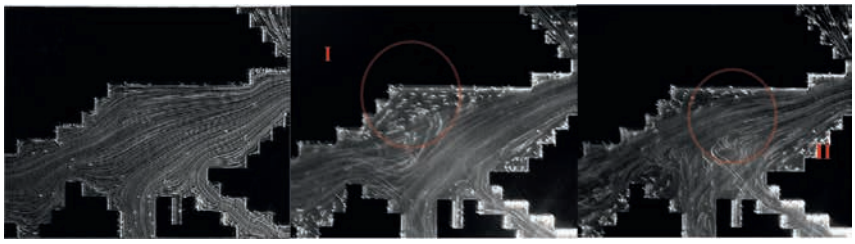

Figure 3 *Flow pattern visualization and comparison between Non-Newtonian polymer solution and brine in Glass-Silicon-Glass micromodels which are resembling a real structure at 100 µl/min; a) 4 g/l brine, b), c) Flopaam 6035s 500 ppm 4g/l Non-Sheared. Photos b) and c) are taken from the same polymer at the same flow rate. By comparing both photos, the turbulent flow can be clearly seen.*

and PTFE Teflon tubings. During flood experiments, a differential pressure sensor (0-30 bar) measures the pressure drop along the model.

Every experiment consists of two steps: firstly, permeability measurement, and secondly, differential pressure measurement and streamline visualization by injecting polymer solutions. The experiments use two different fluid types: a Non-Newtonian fluid, represented by a partially hydrolysed polyacrylamide (HPAM) (Flopaam 6035s provided by SNF Floerger) in aqueous solution, and low-salinity brine represents a Newtonian fluid.

Findings and discussion

Changing the solvent (brines of 0.4 g/L and 4 g/L TDS), polymer concentrations (500 ppm, 1000 ppm and 1500 ppm) as well as the shearing conditions (sheared and non-sheared) (Hincapie, 2015), resulted in a change of relaxation time, which provides a quantity of viscoelasticity under rest. Figure 2 shows a correlation between the viscoelasticity and the proportion of pores showing turbulent flow. We observed that characteristic relaxation time (λ_f) will be higher in three conditions: 1) When brine salinity is low 2) Polymer concentration is high and 3) Polymer solution was not mechanically degraded (sheared). Therefore, under these conditions, the onset of turbulence begins earlier (at lower flow rates) and the proportion of pores showing turbulence becomes higher. The occurring elastic turbulences (which are causing the additional pressure differential) are therefore probably responsible for the shear thickening behaviour.

At similar constant flow rate of 100 µl/min, the HPAM shows a turbulent flow whereas the brine for example shows clearly a laminar flow. Remarkable crossing streamlines (Figure 3c (II)), especially in the wall areas (near grains, black) which initiate a flow direction change, can be seen which mainly characterize the turbulence of the polymer solution. In comparison to brine in Figure 3a and concerning crossing streamlines, there is also more than one flow plane. Depending on the focus, particles are expected to slow down to the models' boundaries. Apart from these main characteristics, the creation of a small vortex in the middle of Figure 3b (I) can be observed which is then immediately interrupted by the fluctuating main flow. Thus, the formation of a vortex in such open pore geometry during turbulent flow of viscoelastic polymers is almost impossible. Vortices during the flood experiments are mainly observed in coves where fluid is effected by the high velocity of the bypassing stream. Concerning flow in the small edges of the grains, there is an additional peculiarity. While the streamlines of brine go deep into the edges, there is nearly no flow in the case of HPAM, but the spread of the main flow is influenced by the smallest distance between the edges.

Conclusion and outlook

Different experiments in GSG micromodels have been conducted for a better understanding of the influence on flow patterns of viscoelastic polymers. By adding tracer to the injected fluids, it is possible to do a precise qualitative analysis of flow behaviour in a homogenous porous media. This pore-scale visualization enables a new insight in elastic turbulence and therefore new insights in shear thickening behaviour. In addition, the qualitative analysis is supported by the results of rheological evaluations. A clear correlation between elastic turbulence at pore-scale and characteristic relaxation time was found. By testing a wide range of different viscoelastic and non-viscoelastic fluids, a contribution on the basic understanding of flow of aqueous polymer solutions, as they are used in EOR applications, is made. Furthermore, the development of a Matlab algorithm will enhance quality of images and analysis.

References

Herbas, J.G., Wegner, J., Hincapie, R.E., Födisch, H., Ganzer, L., Castillo, J.A.D. and Mugizi, H.M. [2015]. Comprehensive Micromodel Study to Evaluate Polymer EOR in Unconsolidated Sand Reservoirs. *SPE Middle East Oil and Gas Show and Conference*. Expanded Abstracts.

Hincapie, R.E. and Ganzer, L. [2015]. Assessment of Polymer Injectivity with Regards to Viscoelasticity: Lab Evaluations towards Better Field Operations. *77th EAGE Conference and Exhibition*, Extended Abstracts.

Ganzer, L., Wegner, J. and Buchebner, M. [2014]. Benefits and Opportunities of a "Rock-on-a-Chip" Approach to Access New Oil. *Oil Gas-European Magazine*, **39**, 43-47.